scientific reports

Check for updates

OPEN

Optogenetic activation of hypothalamic AgRP neurons in transgenic zebrafish larvae increased food intake

Hossein Mehrabi[1,7], Pushkar Bansal[2,7], John Jutoy[1], Yat Ho Chan[3], Mitchell F. Roitman[4], Ruixuan Gao[3,5] & Erica E. Jung[1,6]✉

Agouti Related Peptide (AgRP) neurons are located in the hypothalamus, and upon stimulation, these neurons regulate hunger and hunger-mediated behaviors, especially food-seeking and compulsive eating. AgRP neurons are naturally activated by ghrelin binding onto the ghrelin receptors on the neuron surface during starvation or fasting state to evoke the aforementioned behaviors. In this study, we used channelrhodopsin (ChR2), an optogenetic actuator, to control AgRP neuronal activity. For the first time, we observed food-intake behavior in zebrafish larvae by optogenetically triggering AgRP1 neurons. We created a transgenic line, Tg(AgRP1:ChR2-Kaede), where ChR2-Kaede is expressed in AgRP1 neurons. Transgenic zebrafish Tg(AgRP1:ChR2-Kaede) larvae at 6 days post fertilization and wild-type (ABWT) larvae were used to compare the suction behavior. We found that AgRP1 neuron activation in transgenic larvae led to a significantly higher food-consumption behavior than wildtype larvae when analyzed using Particle Image Velocimetry (PIV) to calculate the food particle velocity initiated by larval suction behavior. These findings in this novel transgenic zebrafish model would be useful in studying various hunger-related behaviors, their underlying neural circuits, and substrates subjected to different chemical stimuli, including drugs of abuse.

Keywords Optogenetic stimulation, AgRP neurons, Zebrafish, Food intake, Suction behavior, Microfluidics devices

Food consumption is essential to sustenance and supports metabolism in animals. Central signaling of hunger is mediated, in part, by neuronal populations in the hypothalamus. In particular, neurons expressing Agouti-related peptide (AgRP) in the arcuate nucleus of the hypothalamus play a major role in controlling appetite, and their activation is sufficient to drive voracious eating[1]. Previous studies reported that AgRP neurons are activated during food restriction leading to an increase in food-seeking and food-intake behavior in rodent using chemogenetic approaches[2]. Other approaches such as optogenetic activation has also been used to activate AgRP neurons and studied its consequent food-consumption behavior in mammals[3]. Optogenetic activation of neurons is a minimal (in rodents and primates)[4,5] to non-invasive (zebrafish, flies and nematodes)[6–8] approach to stimulate a specific population of neurons in animals that involves the incorporation of channelrhodopsin in the neurons. This approach could be useful in gaining insights on functional conservation of AgRP neurons in other species has largely been unexplored.

In this study, we for the first time explored the function of AgRP neurons in zebrafish larvae by optogenetically activating these neurons and examined the resulting changes in food intake behavior. AgRP neuron populations are partially conserved across animals where AgRP neurons in rodents co-express Neuropeptide-Y and are altogether called AgRP/NPY neurons[9], whereas in Zebrafish, AgRP and NPY neurons exist as two distinct entities in separate locations[10]. Previous studies only indirectly suggest the role of AgRP neurons in food intake in zebrafish. For example, a study showed that increased food-intake was higher in control zebrafish

[1]Department of Mechanical Engineering, University of Illinois Chicago, 842 W Taylor St, Chicago, IL 60607, USA. [2]Department of Pharmacology and Toxicology, The University of Utah, 30S 2000E, Salt Lake City, UT 84112, USA. [3]Department of Chemistry, University of Illinois Chicago, 845 W Taylor St, Chicago, IL 60607, USA. [4]Department of Psychology, University of Illinois Chicago, 1007 W Harrison St, Chicago, IL 60607, USA. [5]Department of Biological Sciences, University of Illinois Chicago, 845 W Taylor St, Chicago, IL 60607, USA. [6]Richard and Loan Hill Department of Biomedical Engineering, University of Illinois Chicago, 851 S Morgan St, Chicago, IL 60607, USA. [7]Hossein Mehrabi and Pushkar Bansal contributed equally to this work. ✉email: ejung72@uic.edu

subjects compared to AgRP1 ablated counterparts[11,12]. Moreover, the role of AgRP neurons in feeding behavior in zebrafish by showing the upregulation of AgRP neuron gene expression in fasted larval zebrafish was also recorded[13]. Additionally, oatp1c1 ablation which led to AgRP neuron proliferation resulted in increased food consumption[14]. Taking together the aforementioned research, we hypothesized that optogenetic activation of AgRP1 neurons in zebrafish would lead to an increased food-intake behavior than the wildtype larvae.

Zebrafish larvae are excellent animal models for neuroscience research due to their small size (~3 mm) and optical transparency for observing activities inside the larval body, such as in the brain. Optogenetics has been used in zebrafish larvae to observe brain activity and alter behavior by controlling neuron activity in transgenic lines. In this study, we have created a transgenic Tg(AgRP1:ChR2-Kaede) zebrafish line expressing an excitatory channelrhodopsin ion channel peptide complexed with a fluorescence-emitting protein called Kaede. Both proteins are photoactivatable, and Kaede exhibits a change in color upon photoactivation, confirming the activation of the ChR2-Kaede complex and the neurons. We photoactivated AgRP1 neurons in zebrafish larvae which was partially immobilized in a microfluidic device while feeding the larvae with fish food particles suspended in fish water. Particle Image Velocimetry (PIV) analysis was used to track the motion of the food particles that were being consumed by the larva. Using PIV, we quantified the flow of food particles in terms of food particle motion and velocity calculation in the fish water which was initiated by suction behavior. Our results show that activation of AgRP1 neurons caused a significantly higher food consumption than ABWT larvae. These results indicate that the function of AgRP neurons in different animal species remains conserved despite the absence of an important co-expressing peptide in the same neurons.

Materials and methods

Transgenic line generation

We generated a transgenic zebrafish line Tg(AgRP1:ChR2-Kaede) using Tol2 mediated transgenesis system. A 3 kb long AgRP promotor was used to control the ChR2-Kaede ORF that was fused on its 3′ end. Here, kaede acted as a confirmatory fluorophore to assure the activation of AgRP1 neurons by imaging the color transition from green to maple red upon activation via blue light (470 nm) and the complex has been used earlier[15]. The ChR2-Kaede was tagged into the 3′ end of simian virus 40 (SV40) polyA region. We optically activated the AgRP1 neurons in F2 progeny with blue light to induce the change in food-intake behavior. Additionally, we confirmed the genomic integration of AgRP1 promotor into ChR1-kaede tag and observed the amplification of transgene in the transgenic F2 generation compared to wildtype and NTC control samples.

To validate the genomic integration of the Tg(AgRP1:ChR2-Kaede) transgene, fin clips were collected from F1 zebrafish for genomic DNA (gDNA) extraction. PCR analysis was conducted using two specific primer sets designed to amplify key regions of the construct. Primer pair ZMX3011/ZMX3017 targeted a 1646-bp fragment spanning the 3′ end of the AgRP1 promoter, the ChR2 open reading frame (ORF), and part of the Kaede tag, while primer pair ZMX3016/ZMX3019 amplified an 860-bp region that included the Kaede ORF and the polyA tail. Gel electrophoresis revealed the expected amplicons in transgenic samples, while no amplification was observed in wild-type and no-template controls, confirming the specificity of the transgene insertion (see Supplementary Figs. S1 and S2 online). Sanger sequencing of the PCR products further verified the integrity of the construct. Variation in band intensity among F1 animals was attributed to differences in gDNA quality, insertion site, or transgene copy number.

Zebrafish breeding

We used 6dpf transgenic Tg(AgRP1:ChR2-Kaede) (n = 10, 13) and ABWT (n = 9, 14) zebrafish larvae bred in our fish facility at the University of Illinois at Chicago. Fish were housed in the tanks and placed in a fish rack (Aquaneering, Inc., San Diego, CA). All fish were kept in a 14/10 h light/dark cycle, and the facility was maintained at 27 °C temperature. Experimental larvae were initially raised and placed in the fish facility and transported to the experiment facility once the larvae turned 6 dpf. Larvae were kept deprived of food till 6 dpf since zebrafish larvae can thrive without feeding till 8 dpf with no growth or developmental anomalies[16]. All experimental procedures were conducted in accordance with relevant guidelines and regulations and were approved by the Institutional Animal Care and Use Committee (IACUC) at the University of Illinois Chicago (UIC) under protocol number 24-115. This institution holds Animal Welfare Assurance Number D16-00290 (A3460.01), registered with the Office of Laboratory Animal Welfare, NIH. This study is reported in accordance with the ARRIVE guidelines 2.0.

Microfluidic device design and manufacturing

Individual zebrafish larvae were trapped in an in-lab constructed microfluidic device to monitor and measure the velocity of food particles suspended in fish water. A resin 3D printed positive mold was created with features: liquid input/output, particle flow channel, larva trapping, and water reservoirs. Creation of the device consisted of heating agarose gel into its liquid form and placing it into a petri dish with the positive mold. Mold is removed post-solidification of agarose gel. Liquid input and output were necessary to introduce food particles into the channel via pipette. The channel passes directly through the center of the larva trap to provide larval access to food particles suspended in water. Flow and mouth movements are not obstructed due to the channel geometry, although the larva is immobilized from body movement due to the tapering geometry. Water reservoirs prevented significant water evaporation in the main channel due to the porous nature of agarose. Additionally, the water reservoir feature acted as a spacer for the positive mold to prevent misalignment in the mold creation.

Sample preparation and materials

Individual zebrafish larvae were carefully placed using a transfer-pipette near the microchannel in the microfluidic device. A hair loop was used to move and align the larva into the channel for the desired orientation.

In the microchannel, 0.2 ml of fish water containing fish food particles was dropped near the fish's mouth using a micropipette. The partially immobilized larva in the device is then placed under an upright epifluorescent microscope setup (Olympus Corporation, Japan). Once the sample was placed, the neurons were illuminated, and Kaede expression was checked to confirm activation. The setup consisted of a 10 × air objective (Olympus Corporation, Japan), fluorescence excitation, and illumination setup equipped with a wavelength filter of 488 nm excitation/507 nm emission. Recordings were made using a high-speed sCMOS camera at 33 frames per second connected to HC Image live software (version 4.5.0.0, Hamamatsu Corp., Japan, https://www.hamamatsu.com/).

The area of blue light stimulation was determined by placing a reference object under the microscope at the same focal plane as the experiments. The illuminated area was captured and analyzed using ImageJ (version 1.53e, National Institutes of Health, USA, https:// https://imagej.net/ij/), with the same calibration references used for experimental videos. The stimulation diameter was measured as 2.471 mm, corresponding to a circular area of approximately 4.8 mm^2. The power of blue light was measured with a ThorLabs PM100D optical power meter and S175C sensor, with power ranging from 75 to 105 mW during experiments. The blue light (470 nm) was applied continuously for 1 min to activate AgRP1 neurons. Pulsed stimulation was not used because changes in light intensity interfered with the camera's ability to detect food particles during video recording.

For imaging Tg(AgRP1:ChR2-Kaede) transgenic zebrafish larvae, samples were embedded in 1.5% low-melting-point agarose using transfer pipettes. Larvae were first imaged under an upright epifluorescent microscope equipped with a 20 × water-immersion objective. Subsequently, the same larvae were imaged using a Yokogawa spinning-disk confocal system (CSU-W1) mounted on a Nikon Eclipse Ti2-E microscope. Confocal imaging was performed using a 488 nm solid-state laser and a 40 × 1.15 NA water-immersion objective.

Post-processing

Recorded videos were converted into individual frames using ImageJ and were exported into a third-party MATLAB (version R2020a Update 8 (9.8.0.1873465), MathWorks, USA, https://www.mathworks.com/) application called PIV lab[17](version 2.63, http://PIVlab.de/). Following appropriate suggested steps and parameters in the application, including masking, contrast correction, calibration, image, and velocity validations, we analyzed the velocity of the food particles that were being sucked in by the larvae. A 200 × 200 μm^2 area was selected right next to the larva mouth in which the velocity of the tracked particles was measured and saved as a note file that consisted of frame versus velocity data. Suction events were quantified using the processed velocity versus frame data obtained from PIV lab. Peak regions with the highest velocities were identified as suction events using the Peak Analyzer tool in Origin (Version 2022, OriginLab Corporation, Northampton, MA, USA, https://www.originlab.com/) with the following parameters: Asymmetric Least Square Smoothing method, asymmetric factor of 0.01, threshold of 0.25, smoothing factor of 2, 40 iterations, and local points of 10. The results were validated using ImageJ by placing a vertical line in front of the larva's mouth and counting half the number of times the mouth crossed the line as the number of suctions.

Statistical analysis

All data were preprocessed using Origin with baseline subtraction performed via the Asymmetric Least Square Smoothing method. The following parameters were applied: asymmetric factor of 0.01, threshold of 0.25, smoothing factor of 2, and 40 iterations. Subsequent analyses were conducted in Python 3. Outliers in each dataset were identified and removed from the statistical analysis using the interquartile range (IQR) method, where values outside the lower whisker (Q1 – 1.5 * IQR) and upper whisker (Q3 + 1.5 * IQR) were excluded. This approach was chosen to prevent extreme values, arising from experimental noise or rare variability, from artificially influencing the statistical analysis. While behavioral parameters are typically normally distributed, occasional outliers were excluded to enhance the robustness of the analysis and ensure reliable conclusions.

For the analysis of mean velocity, mean suction frequency, and their product, the Shapiro–Wilk test was used to assess the normality of differences between baseline and stimulation values. Paired t-tests were used for normally distributed data with homogeneous variance; otherwise, the Wilcoxon signed-rank test was applied. To evaluate absolute differences in mean velocity, mean suction frequency, their product, and baseline activity comparison between the ABWT and Tg(AgRP1:ChR2-Kaede) groups, normality was again assessed using the Shapiro–Wilk test. Independent t-tests were performed when both groups were normally distributed with homogeneous variance, while the Mann–Whitney U test was applied if the criteria for the independent t-test were not met by one or both groups. For baseline activity comparisons across groups, p-values were adjusted using the Bonferroni correction to account for multiple comparisons. Statistical significance was defined as follows: n.s. (not significant) for $p > 0.05$, * for $p < 0.05$, ** for $p < 0.01$, *** for $p < 0.001$, and **** for $p < 0.0001$.

Results

Creation of transgenic line Tg(AgRP1:ChR2-Kaede)

To investigate the functional role of AgRP1 neurons in zebrafish, we have utilized the Tol2 transgenesis system to generate a transgenic line that expresses ChR2-kaede under the transcriptional control of the AgRP1 promoter, permitting specific photoactivation of AgRP1 neurons by blue light illumination (Fig. 1a). In Fig. 1b, we depicted a crossing scheme yielding heterozygous F2 progeny, which were used for all subsequent analyses. To validate the targeting of AgRP1 neurons, a Tg(AgRP1:ChR2-Kaede) transgenic larva was embedded in 1.5% low-melting-point agarose and imaged under an upright epifluorescent microscope using a 20 × water-immersion objective. Kaede fluorescence was detected in the approximate anatomical location of AgRP1 neurons (Fig. 1c). The same larva was subsequently imaged using a confocal microscope with a 40 × water-immersion objective (Fig. 1d), revealing five labeled AgRP1 neurons. Typically, 6 dpf zebrafish larvae possess approximately 10–20 AgRP1 neurons[14]. In our transgenic line, the number of labeled neurons varies across individual larvae, ranging from

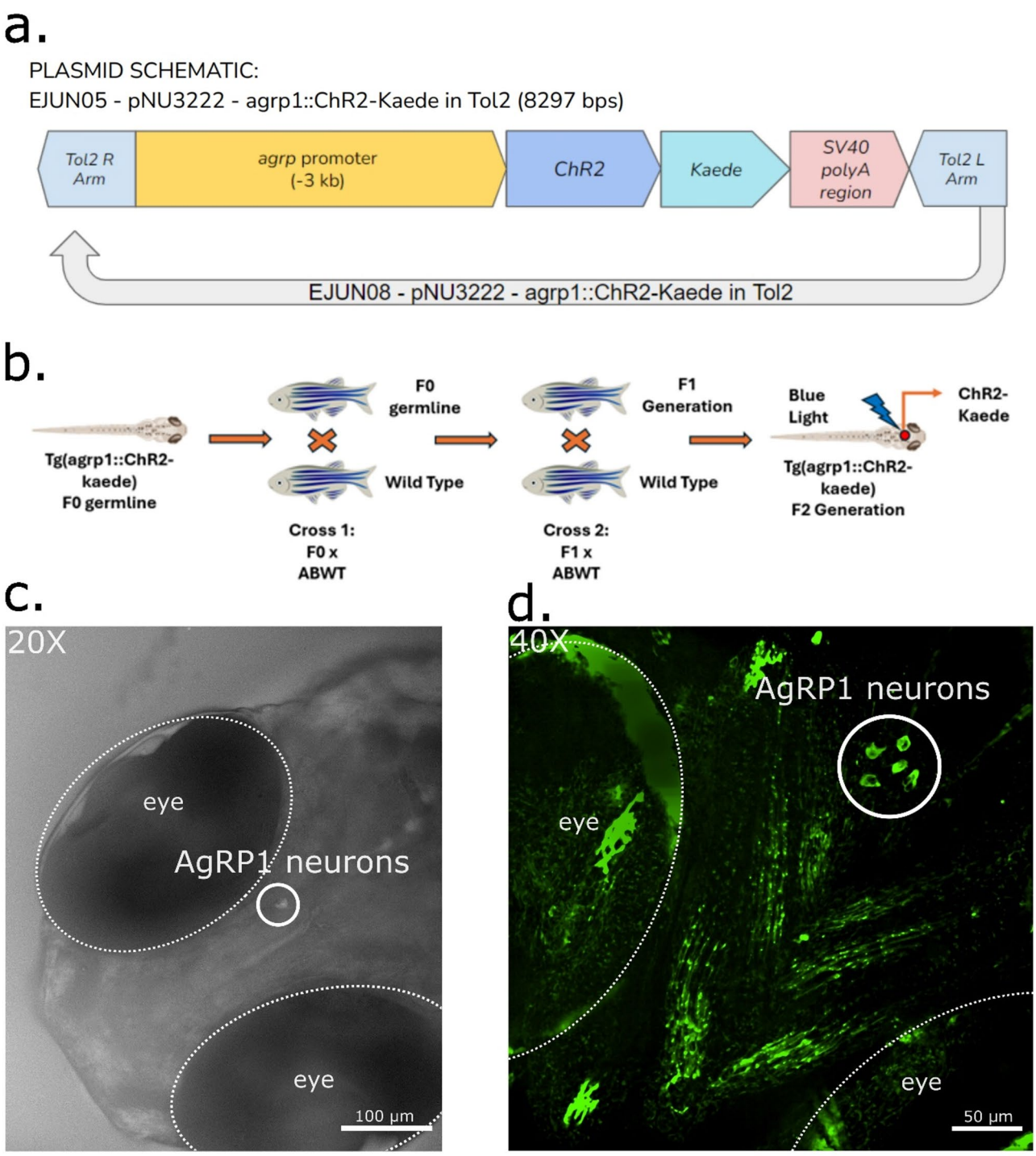

Fig. 1. (**a**) Schematic of the Tol2 transgenic construct used to generate zebrafish expressing ChR2-Kaede under the control of the AgRP1 promoter. (**b**) Breeding strategy to generate heterozygous F2 transgenic larvae, which were subsequently stimulated with blue light to activate AgRP1 neurons. (**c**) Screening of a Tg(AgRP1:ChR2-Kaede) larva under an upright epifluorescent microscope using a 20 × water-immersion objective. The approximate anatomical location of AgRP1 neurons is indicated relative to the eyes. (**d**) High-magnification confocal imaging of the same larva using a 40 × water-immersion objective, showing five AgRP1 neurons labeled by endogenous Kaede fluorescence.

as few as one neuron to labeling of nearly the entire AgRP1 neuronal population (see Supplementary Figs. S1 and S2 online).

Suction behavior analysis

To facilitate experiments in feeding behavior, we designed custom microfluidic chambers capable of precision control over food particle flow as well as optogenetic activation of AgRP1 neurons. The mold shown in Fig. 2a was first fabricated using 3D printed resin. Then, the agarose negative mold represented in Fig. 2b was created from the resin mold and used to observe suction behavior through the microchannel, as shown in Fig. 2c. Zebrafish larvae were orientated towards the center of the device with their mouths facing the flow of food particles (Fig. 2d). We used an epifluorescent microscope to optogenetically activate AgRP1 neurons (blue light stimulation at 470 nm; Fig. 2e,f). To analyze food suction behavior, we partially immobilized larvae in a microfluidic channel and used Particle Image Velocimetry (PIV) to track food particle movement towards the larvae's mouth (Fig. 3). A zoomed-out view of the trapped larvae is shown in Fig. 3a, with a close-up in Fig. 3b. PIV analysis revealed the flow of food particles during suction and represented with vector fields (Fig. 3c). We recorded food suction behavior in baseline conditions (without blue light stimulation) for 1 min, and followed by the blue light stimulation to activate AgRP1 neurons. Figure 3d and Fig. 3e shows particle sucked through the microchannel under baseline conditions and during the AgRP1 neuron optogenetic stimulation with blue light, respectively (see Supplementary Video S1, S2, S3, and S4 online).

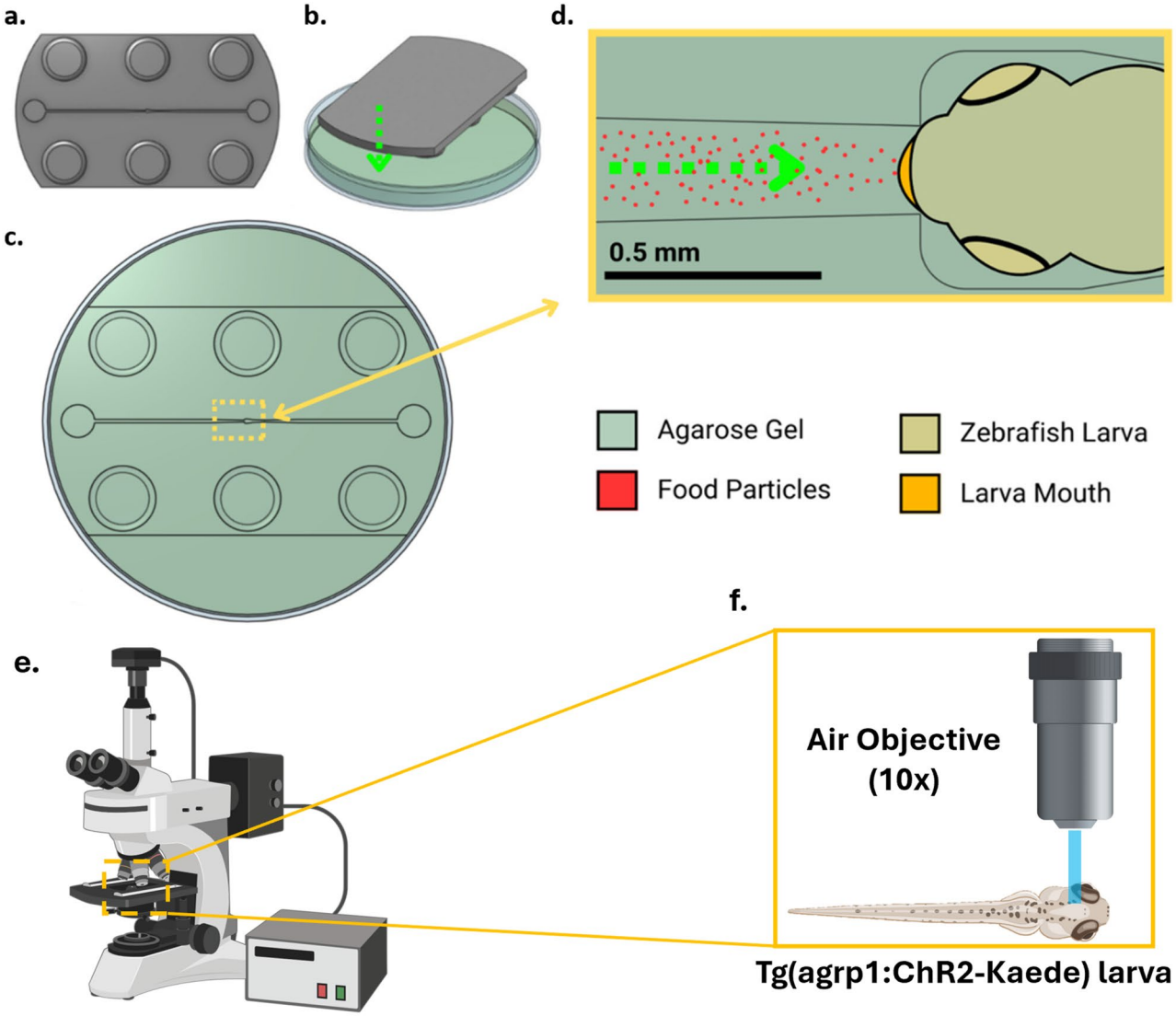

Fig. 2. Microfluidic Chamber and Optogenetic activation. A resin 3D printed positive mold (**a**) was designed to create a negative mold in liquid agarose (**b**) inside a petri dish. The negative mold of solidified agarose (**c**) acts as reusable device for food particle flow experiments. Zebrafish larva can be placed and trapped in the center of the device (**d**) while having mouth access to food particles suspended in water. (**e**) In an Olympus BX51 fluorescence microscope (**f**) a 10 × magnification air objective was used to photoactivate the AgRP1 neurons in the hypothalamus of the larva by delivering blue light stimulation at a wavelength of 470 nm.

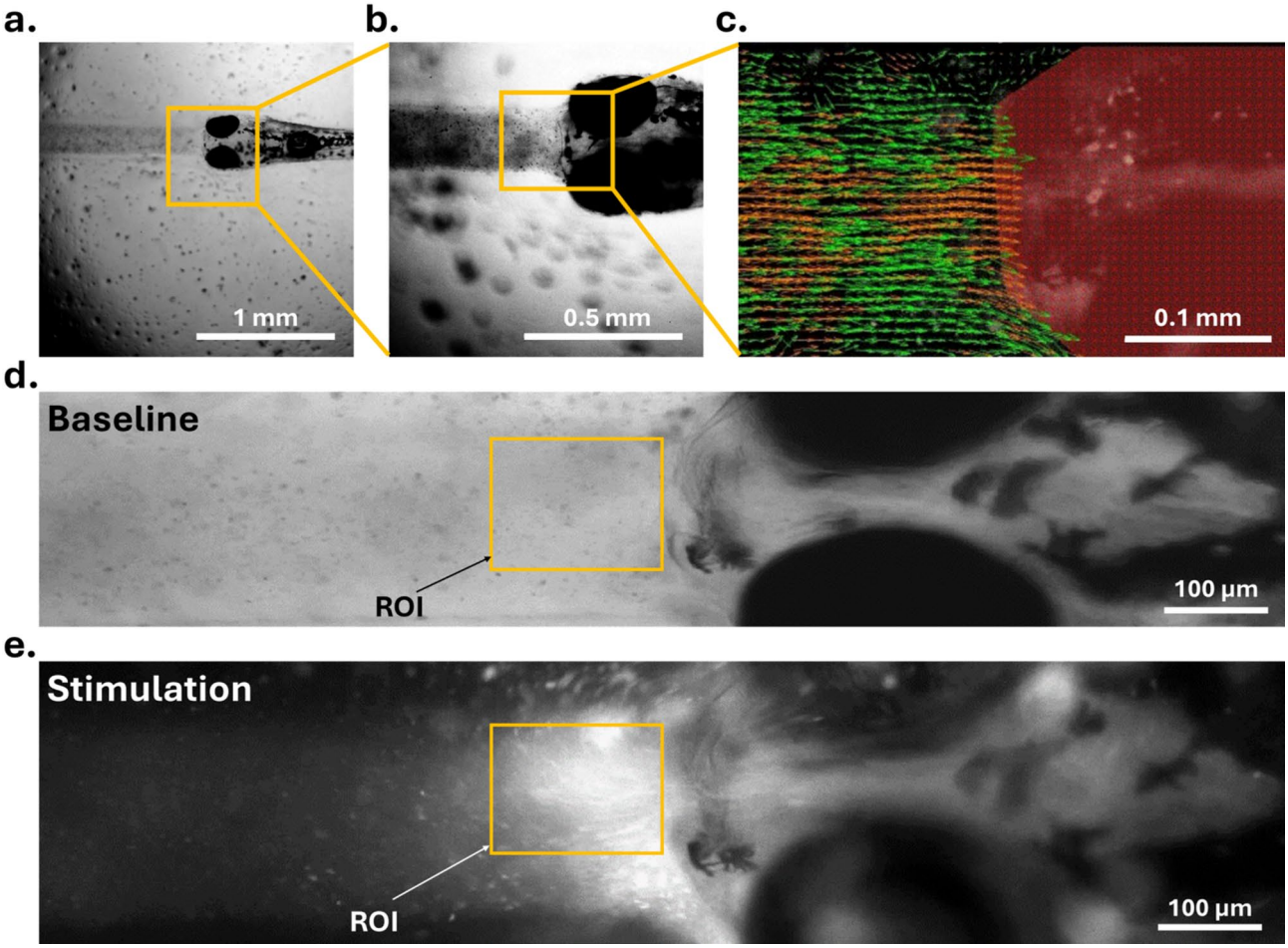

Fig. 3. Larval entrapment and PIV analysis. Larvae was partially immobilized in a microfluidic channel and food suction behavior was analyzed using Particle Image Velocimetry (PIV). (**a**) Zoomed-out view of the trapped larva with the mouth facing toward the channel. (**b**) Zoomed in view of the immobilized larva. (**c**) Food particles flowing toward the fish mouth via larval food consumption behavior are represented with vectors. (**d**) Food suction behavior was recorded first without the stimulation (baseline) and with the selected ROI. (**e**) Post-stimulation of AgRP1 neurons and representation of food-intake.

Baseline comparison across groups

We used four groups of zebrafish larvae: ABWT (Fed ad libitum and Food-Deprived), serving as the wild-type control group, and Tg(AgRP1:ChR2-Kaede) (Fed ad libitum and Food-Deprived), a transgenic line in which AgRP1 neurons can be optogenetically stimulated. Also, all samples in Fed groups were fed ad libitum starting 4 days post fertilization. For each sample in the ABWT and Tg(AgRP1:ChR2-Kaede) groups, we recorded data for 1 min at 33 fps during both baseline and stimulation phases, capturing the mean velocity magnitude of the region of interest (ROI) for each frame. From these data, we calculated an average velocity for the baseline and stimulation phases of each sample. Additionally, the suction distribution was derived from the velocity profile of each sample.

To examine baseline velocity and suction frequency in Fed ad libitum and Food-Deprived ABWT and Tg(AgRP1:ChR2-Kaede) groups, a direct comparison was conducted (Fig. 4). As expected, overall activity (velocity and suction frequency) was higher in Fed groups compared to Food-Deprived groups, likely due to their higher energy levels from recent feeding. There were no significant differences in velocity between the four groups. However, suction frequency showed significant differences between Fed ABWT and FD ABWT (p-value = 0.02942), Fed AgRP and FD ABWT (p-value = 0.00583), and Fed AgRP and FD AgRP (p-value = 0.04784). All significant differences occurred between a Fed ad libitum group and a Food-Deprived group, likely due to differences in energy levels. In subsequent analyses, comparisons were restricted to either two Fed ad libitum groups or two Food-Deprived groups, as there were no significant differences in baseline activity between these conditions.

Optogenetic stimulation of AgRP1 in zebrafish larvae

Figure 5 illustrates the velocity dynamics, mean velocity, mean suction frequency, and their product in the fed ad libitum ABWT and Tg(AgRP1:ChR2-Kaede) groups. In the ABWT group, velocity traces were relatively evenly

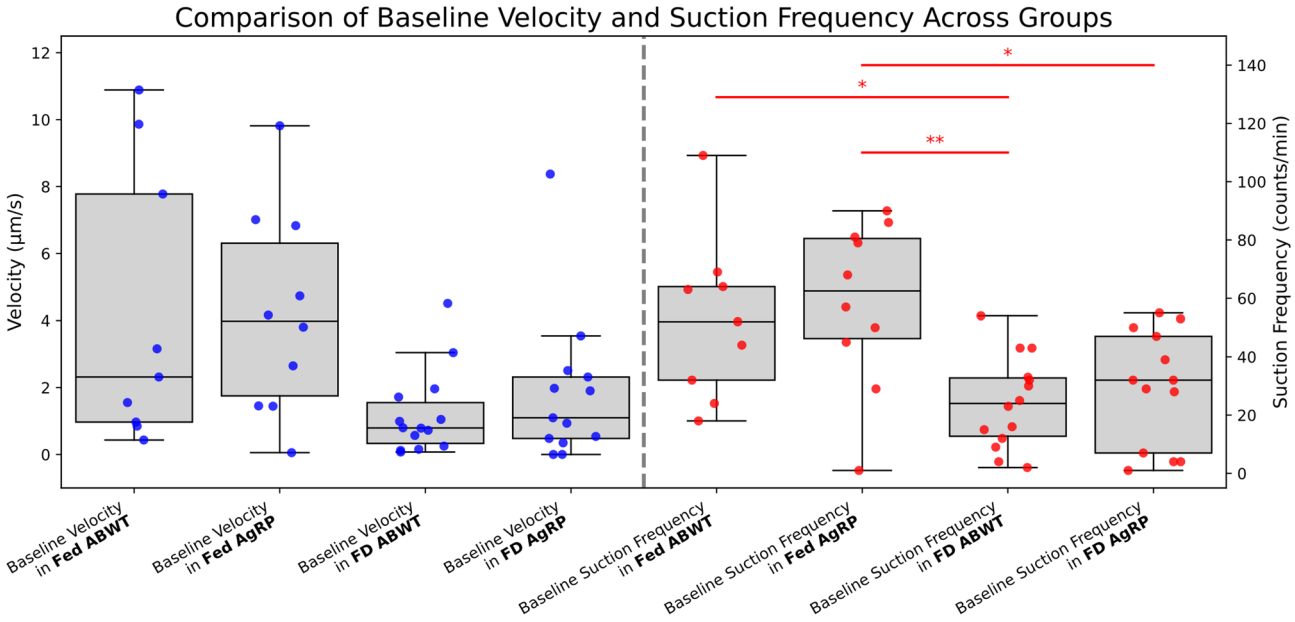

Fig. 4. Comparison of Baseline Velocity and Suction Frequency Across Fed and Food-Deprived Conditions in ABWT and Tg(AgRP1:ChR2-Kaede) Groups. Boxplots show the distribution of baseline velocity (left panel, blue) and suction frequency (right panel, red) in each condition, with individual data points displayed for each group. These analyses underscore the differences in baseline suction frequency between fed and food-deprived states, providing important context for the hunger-dependent behavioral changes observed during stimulation. Statistical comparisons were conducted using independent t-tests, with the following *p*-values: Fed ABWT versus FD ABWT, $p = 0.02942$; Fed AgRP versus FD ABWT, $p = 0.00583$; Fed AgRP versus FD AgRP, $p = 0.04784$.

distributed across the baseline and stimulation phases, with no marked increase in activity during stimulation (Fig. 5a). In contrast, some of the samples in the Tg(AgRP1:ChR2-Kaede) group displayed a pronounced increase in velocity immediately following stimulation (Fig. 5b), while few samples did not exhibit a significant increase, likely due to variability in AgRP1 neuron labeling and ChR2 expression levels, as the number of targeted AgRP1 neurons can vary across larvae in our transgenic line (see Supplementary Figs. S1 and S2 online). The average velocity over time appeared similar between the two groups; however, the Tg(AgRP1:ChR2-Kaede) group displayed a relatively higher increase after stimulation, although this may not be a reliable criterion for group comparison, as the velocity magnitude remained near zero during most time frames for the majority of samples. The dashed red line at 60 s indicates the transition from baseline to stimulation. The maximum velocity of each sample is shown next to its normalized velocity profile.

To evaluate the effects of optogenetic stimulation in our two groups, we analyzed the average velocity during baseline and stimulation phases for each sample. In both the ABWT and Tg(AgRP1:ChR2-Kaede) groups, no significant changes in mean velocity were observed between baseline and stimulation phases (Fig. 5c, *p*-value: 0.63711; Fig. 5d, p-value: 0.10514). To further investigate potential differences between the two groups, we calculated the absolute differences in mean velocity between the two phases. This analysis revealed no statistically significant difference between the groups (Fig. 5e, *p*-value: 0.33886).

Next, we assessed suction frequency, an additional parameter indicative of feeding behavior, across baseline and stimulation phases. In the ABWT group, suction frequency remained stable, showing no significant changes between phases (Fig. 5f, *p*-value: 0.41470). In contrast, the Tg(AgRP1:ChR2-Kaede) group exhibited a significant increase in suction frequency during stimulation (Fig. 5g, *p*-value: 0.00227). When comparing the absolute differences in suction frequency between baseline and stimulation, the Tg(AgRP1:ChR2-Kaede) group displayed significantly greater changes than the ABWT group (Fig. 5h, *p*-value: 0.02424).

To capture an integrated view of feeding dynamics, we calculated the product of mean velocity and suction frequency as an estimate of total food intake. The product of mean velocity times cross-sectional area is a volumetric flow rate Q[18] and since the cross-sectional area of the microchannel is constant, the product of mean velocity and suction frequency is proportional to the total food intake. In the ABWT group, this parameter did not significantly vary between baseline and stimulation phases (Fig. 5i, *p*-value: 0.68047). However, the Tg(AgRP1:ChR2-Kaede) group showed a significant increase in this combined parameter during stimulation (Fig. 5j, *p* value: 0.02265). Despite this, the comparison of absolute differences in the combined parameter between the two groups did not exhibit statistical significance (Fig. 5k, *p* value: 0.08214), suggesting that the overall feeding response was not markedly different between the groups.

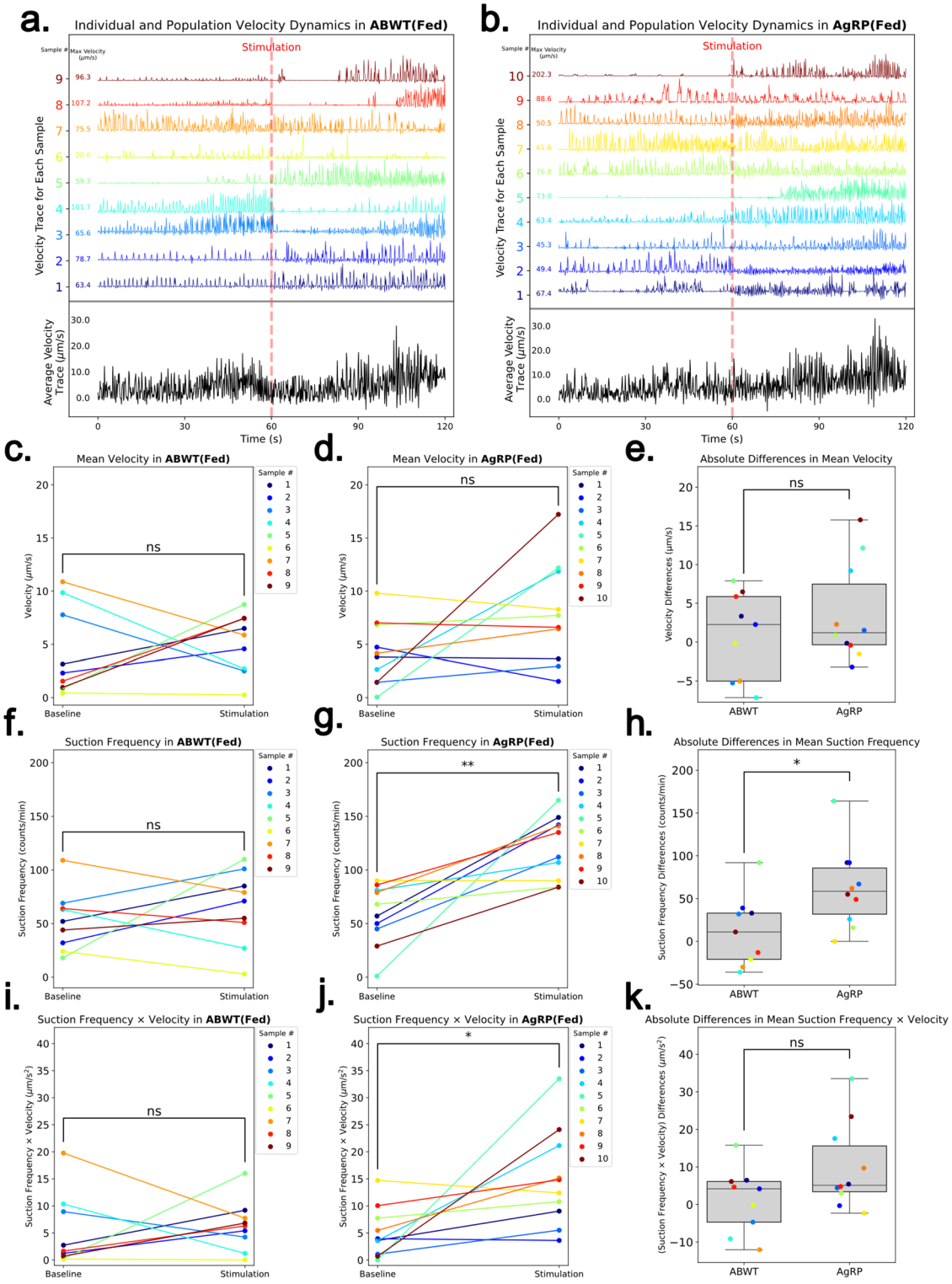

Impact of hunger on feeding behavior in zebrafish larvae

To assess the influence of hunger on feeding behavior and its potential modulation by AgRP neurons, we conducted an additional series of experiments. In this experiment, both the Tg(AgRP1:ChR2-Kaede) and ABWT groups kept food deprived since birth until the experiment on 6 days post fertilization. Unlike the previous series where larvae were fed ad libitum starting 4 dpf, these experiments aimed to determine how feeding status impacts the neuronal and behavioral responses to stimulation.

Figure 6a illustrates normalized velocity traces for individual samples and the average of all samples in the ABWT group, while Fig. 6b shows the same for the Tg(AgRP1:ChR2-Kaede) group. In the ABWT group, velocity dynamics remained relatively uniform across the baseline and stimulation phases, with no marked shift in timing or frequency of events. This pattern suggests a consistent feeding behavior that remains largely unchanged by stimulation in majority of samples. This suggests that food deprivation prior to testing did not

◀**Fig. 5**. Analysis of velocity dynamics, mean velocity, mean suction frequency, and their product in ABWT and Tg(AgRP1:ChR2-Kaede) Groups During Fed (ad libitum) Experiment. (**a**, **b**): Normalized velocity traces for individual samples and the average of all samples in the ABWT (**a**) and Tg(AgRP1:ChR2-Kaede) (**b**) groups during baseline and stimulation phases. The dashed red line at 60 s indicates the transition from baseline to stimulation. The maximum velocity for each individual sample over the 120-s period is displayed alongside each sample's plot. (**c, d**) Mean velocity in the ABWT (**c**) and Tg(AgRP1:ChR2-Kaede) (**d**) groups across baseline and stimulation phases, showing no significant change during the stimulation in both groups (paired t-test, *p*-values: 0.63711 for ABWT, 0.10514 for Tg(AgRP1:ChR2-Kaede)). (**e**) Boxplot of absolute differences in mean velocity between the ABWT and Tg(AgRP1:ChR2-Kaede) groups, showing no significant difference (independent t-test, *p*-value: 0.33886). (**f**, **g**) Suction frequency in ABWT (**f**) and Tg(AgRP1:ChR2-Kaede) (**g**) groups, showing no significant change in ABWT (paired t-test, *p*-value: 0.41470) but a significant increase in Tg(AgRP1:ChR2-Kaede) during stimulation (paired t-test, *p*-value: 0.00227). (**h**) Boxplot of absolute differences in suction frequency, with the Tg(AgRP1:ChR2-Kaede) group exhibiting significantly greater changes compared to ABWT (independent t-test, *p*-value: 0.02424). (**i**, **j**) Combined analysis of suction frequency and velocity in ABWT (**i**) and Tg(AgRP1:ChR2-Kaede) (**j**) groups, indicating no significant difference in ABWT (paired t-test, *p*-value: 0.68047) but a significant increase in Tg(AgRP1:ChR2-Kaede) following stimulation (paired t-test, *p*-value: 0.02265). (**k**) Boxplot of absolute differences in the product of suction frequency and velocity between ABWT and Tg(AgRP1:ChR2-Kaede) groups, showing no significant difference (independent t-test, *p*-value: 0.08214).

substantially alter the velocity dynamics, reflecting consistent feeding behavior in the lack of a feeding stimulus in most individual samples.

In contrast, the Tg(AgRP1:ChR2-Kaede) group exhibits a distinct temporal pattern, with a notable increase in velocity immediately following the stimulation onset (Fig. 6b) in most samples. However, in sample 10, the velocity decreased upon stimulation, which may be attributed to insufficient ChR2 expression in this sample (see Supplementary Figs. S1 and S2 online). This increased activity during the stimulation phase indicates an adaptive feeding response specific to the Tg(AgRP1:ChR2-Kaede) group. This heightened activity during the stimulation phase mirrors the pattern observed in fed ad libitum Tg(AgRP1:ChR2-Kaede) larvae, although the response appears more intense. The dashed red line at 60 s marks the transition from baseline to stimulation, highlighting a temporal shift and increased velocity during stimulation. These differences between the ABWT and Tg(AgRP1:ChR2-Kaede) groups underscore the unique feeding dynamics elicited by stimulation in the Tg(AgRP1:ChR2-Kaede) group, consistent with previously observed changes in mean velocity and suction frequency.

We compared the baseline and stimulation phases in terms of average velocity to assess the effects of optogenetic stimulation. In the ABWT group, there was no significant change in average velocity between baseline and stimulation. In contrast, the Tg(AgRP1:ChR2-Kaede) group demonstrated a significant increase in average velocity following stimulation (Fig. 6c and d; *p*-values: 0.89002 and 0.00851, respectively). To quantify these changes more precisely, we calculated the absolute differences in mean velocity between the two phases for each sample. In the ABWT group, values clustered around zero, indicating minimal change post-stimulation (Fig. 6e). However, in the Tg(AgRP1:ChR2-Kaede) group, differences were mostly positive and broadly distributed, reflecting a significant increase in velocity. This suggests an enhanced response to stimulation in the Tg(AgRP1:ChR2-Kaede) group compared to ABWT (*p*-value: 0.00972).

To further investigate feeding behavior, we quantified the average suction frequency by counting the number of suctions during baseline and stimulation phases. Suction frequency showed no significant change in the ABWT group (Fig. 6f, *p* value: 0.64880), while the Tg(AgRP1:ChR2-Kaede) group exhibited a significant increase during stimulation (Fig. 6g, *p* value: 0.00134). Absolute differences in suction frequency confirmed this trend, with ABWT values centered around zero, indicating minimal change (Fig. 6h), and Tg(AgRP1:ChR2-Kaede) values consistently positive, reflecting a significant increase in feeding behavior (*p*-value: 0.00169).

In the ABWT group the combined analysis of suction frequency and velocity remained stable across baseline and stimulation phases (Fig. 6i, *p* value: 0.94646), whereas in the Tg(AgRP1:ChR2-Kaede) group, it significantly increased following stimulation (Fig. 6j, *p* value: 0.00447), suggesting that in a food-deprived state, the Tg(AgRP1:ChR2-Kaede) group exhibited a measurable response to stimulation, which was amplified compared to their fed ad libitum state. Absolute differences in this combined parameter further highlighted the distinct response of the Tg(AgRP1:ChR2-Kaede) group, with ABWT samples near zero and Tg(AgRP1:ChR2-Kaede) samples showing marked increases (Fig. 6k), underscoring the amplified feeding dynamics elicited by stimulation in the Tg(AgRP1:ChR2-Kaede) group (*p*-value: 0.00287).

Discussion

Optogenetic actuators have been widely adopted in neuroscience to study how different neuronal populations communicate to induce behavior[19]. In particular, zebrafish larvae, with their transparent bodies and brains, provide an excellent model for adapting optogenetic tools to investigate neural function and behavior. This study investigated the function of AgRP1 neurons by developing a transgenic Tg(AgRP1:ChR2-Kaede) zebrafish line where AgRP1 neurons activity is controlled by the optogenetic actuator, ChR2. For the first time, we showed that activating hypothalamic AgRP1 neurons in zebrafish larvae has evoked a significantly high food-intake behavior.

In zebrafish, food consumption requires jaw and mouth movements to generate suction flows near their mouths, which arise from trigeminal nerves in developing zebrafish which are a part of solitary tract[20,21]. Solitary tract and its functionality as taste sensors is conserved between mammals and zebrafish and palatability of

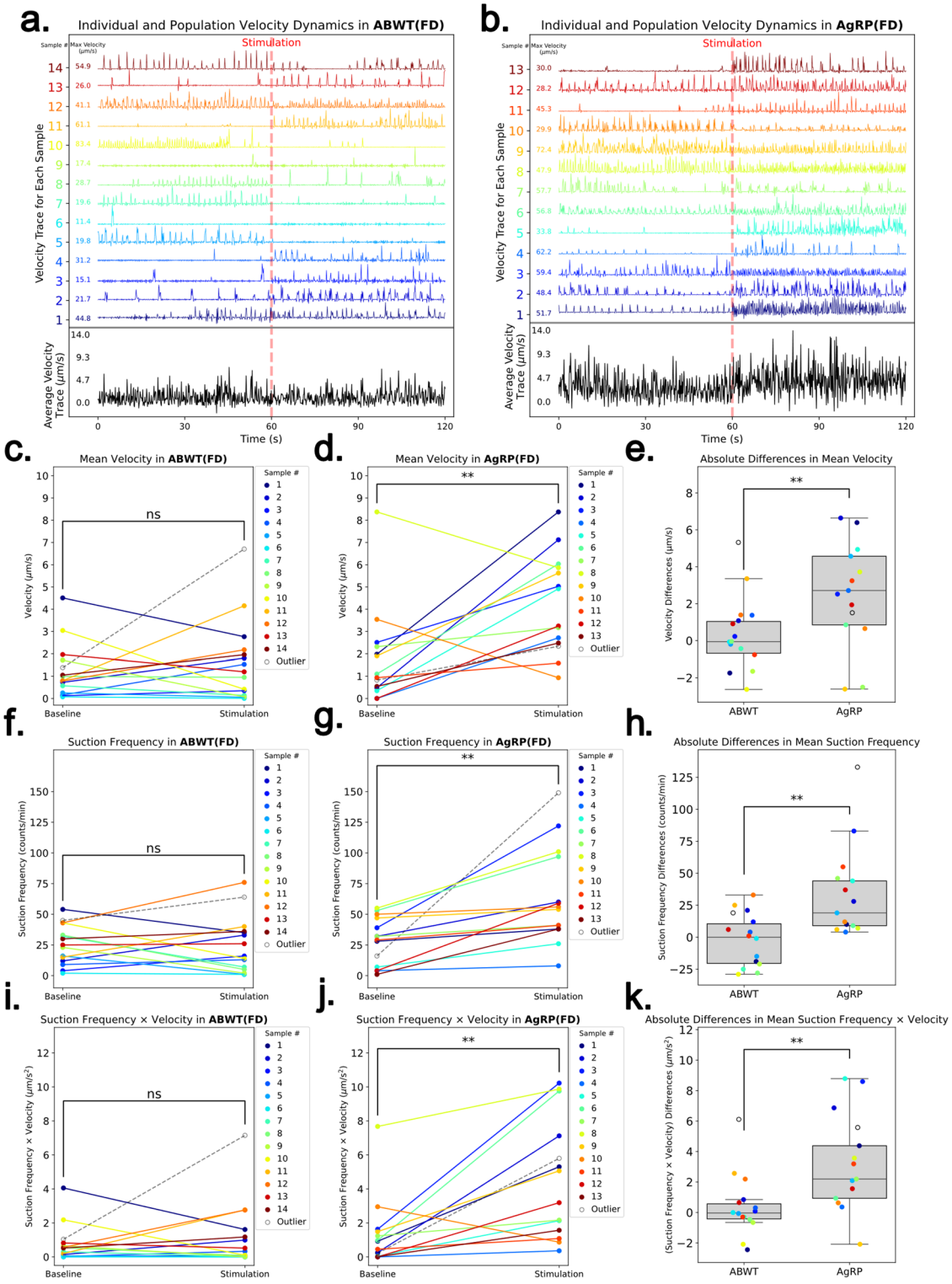

food has been shown to drive feeding independent of AgRP neuron activation in mice[22,23]. In our findings, we observed a significant increase in suction frequency in eating behavior in both fasted and fed states whereas the changes in velocity and suction volume were significant in fasted state only. The suction frequency is a function of solitary tract-dependent jaw and facial movement of the animal. Thus, in fed state the increase in food suction frequency could have been induced due to solitary tract-mediated taste sensing and a probable palatability of the food. Whereas a significantly high jaw motion-mediated suction that was observed fasted state could be a result both AgRP1 activation and solitary tract taste sensing altogether. This does require further research to explore how palatability of food and AgRP1 neurons drive feeding while the neurons are subjected to optogenetic activation.

The findings of this study confirming the involvement of AgRP1 neuron population in food-consumption behaviors in zebrafish is in line with the outcomes observed previously[24]. Unlike mammals, zebrafish have two

◀**Fig. 6**. Analysis of velocity dynamics, mean velocity, mean suction frequency, and their product in food-deprived (FD) ABWT and Tg(AgRP1:ChR2-Kaede) Groups During Baseline and Stimulation Phases. (**a**, **b**) Normalized velocity traces for individual samples and the average of all samples in the ABWT (**a**) and Tg(AgRP1:ChR2-Kaede) (**b**) groups during baseline and stimulation phases. The dashed red line at 60 s indicates the transition from baseline to stimulation. The maximum velocity for each individual sample over the 120-s period is displayed alongside each sample's plot. (**c**, **d**) Mean velocity of baseline and stimulation phases in ABWT (**c**) and Tg(AgRP1:ChR2-Kaede) (**d**) groups, with no significant difference between phases in ABWT (paired t-test, *p*-value: 0.89002) and a significant increase in Tg(AgRP1:ChR2-Kaede) (paired t-test, *p*-value: 0.00851). (**e**) Boxplot of differences in mean velocity of stimulation and baseline between ABWT and Tg(AgRP1:ChR2-Kaede) groups, showing a significantly higher difference in the Tg(AgRP1:ChR2-Kaede) group (independent t-test, *p*-value: 0.00972). (**f**, **g**) Suction frequency in ABWT (**f**) and Tg(AgRP1:ChR2-Kaede) (**g**) groups, with no significant change in ABWT (paired t-test, *p*-value: 0.64880) and a significant increase in Tg(AgRP1:ChR2-Kaede) (paired t-test, *p*-value: 0.00134) during stimulation. (**h**) Boxplot of absolute differences in suction frequency of baseline and stimulation, indicating significantly higher values for Tg(AgRP1:ChR2-Kaede)than ABWT (independent t-test, *p*-value: 0.00169). (**i**, **j**) Product of suction frequency and velocity in ABWT (**i**) and Tg(AgRP1:ChR2-Kaede) (**j**) groups, with no significant change in ABWT (paired t-test, *p*-value: 0.94646) and a significant increase in Tg(AgRP1:ChR2-Kaede) (paired t-test, *p*-value: 0.00447) during stimulation. (**k**) Boxplot of absolute differences in the product of suction frequency and velocity between ABWT and Tg(AgRP1:ChR2-Kaede)groups, showing significantly higher values in the Tg(AgRP1:ChR2-Kaede) group (independent t-test, *p*-value: 0.00287).

distinct AgRP populations AgRP1 and 2, however, only AgRP1 has been found to induce an increase in food consumption whereas AgRP2 contributes to mediating stress response[11]. Interestingly, only one study attempted to explore the synaptic connection between these AgRP populations in zebrafish[25] but only up to the possible observation of AgRP2 innervating AgRP1 populations. This observation calls for the detailed exploration of the functional connection between the populations which is essential to understand the complete synaptic pathway underlying the food intake and seeking dynamics in general as well as in stressful conditions. Additionally, ghrelin a gut hormone which is released during fasting binds to the receptors in AgRP neurons and stimulates them[26]. Ghrelin release and its function is conserved in general[13], however, it is still unclear whether both AgRP populations in zebrafish have ghrelin receptors on their surfaces. Exploring the presence of these receptors on AgRP populations in zebrafish could be another potential topic of future research.

In mammals, besides releasing Agouti related peptide, AgRP neurons also co-express Neuropeptide Y (NPY) and both are an integral part of the mammalian feeding circuitry[27]. AgRP/NPY co-expressing neurons are activated in fasted state and both AgRP and NPY induce rapid feeding[28,29]. In Zebrafish, NPY expressing neurons are present as a separate entity and are not co-expressed with AgRP1/AgRP2 however, similar to mammals, NPY does act as an orexigenic factor in the fish and increase food intake along with AgRP1 only[30,31]. Thus, the functionality of NPY in feeding regulation remains intact between mammals and this teleost. In this study, although not studied, from above-stated research we could speculate the active role of NPY in increased food-intake behavior observed actively in fasted larvae relative to fed larvae. Furthermore, the presence of AgRP and NPY neuron populations as two distinct entities could also have affected the evoked response in fed fish compared to fasted fish when AgRP1 neurons could be pre-active due fasting. The feeding behavior in the zebrafish larva can be observed in future as a response to optogenetic activation of AgRP1 and/or NPY. Channelrhodopsin takes less than 1 ms to get activated upon light stimulation[32] whereas AgRP1 neuron activation in zebrafish has not been explored yet. Here, recording the activation of AgRP1 neurons in conjunction with optogenetic activation of ChR2 is not feasible. Thus, with this limitation, we concluded the activation of the neurons from the feeding behavior of the larva.

We also developed a novel agarose-based microfluidic device designed to restrict the movement of zebrafish larvae during experiments and measure the food particles flowing through the microchannel into their mouths. Our device allows us to observe the feeding related behavior in larvae with minimal to no body motion and only allows the jaw to generate suction flows through the microchannel, similar to sucking through a straw, for food intake. Previously, different types of microfluidic channels, primarily based on PDMS, were designed to restrict the movement of zebrafish larvae[33]. Our in-house developed agarose-based device features a minimalistic design, simple fabrication steps, and a favorable environment created from agarose gel, offering advantages over other PDMS-based microfluidic devices with significantly low manufacturing cost. The suction flow generated through the microfluidic channel was analyzed by tracking individual food particles using the Particle Image Velocimetry (PIV) method[34].

PIV is a conventional technique in fluid mechanics for analyzing flow velocity fields. For example, researchers have used Micro-PIV analysis to analyze waterflow using zebrafish larvae and embryos in microfluidic devices[35–37]. It has also been adapted to study the suction behavior of zebrafish in a reservoir[38]. However, previous studies were limited to the analysis of autonomous feeding without brain stimulation[38]. Using PIV in our study is a novel attempt made to integrate engineering with optics and neurobiological research which resulted in a successful outcome in observing behavior indirectly by analyzing fluid flow arising from optically stimulating neurons located deep inside the animal brain.

Conclusions

In this study, we have investigated the functional role of AgRP1 neurons located in the hypothalamus of zebrafish larvae by developing a transgenic zebrafish line. We incorporated an optogenetic actuator ChR2, a

photoactivatable ion channel complexed with a photo-sensitive fluorescence emitting protein Kaede to confirm neuron activation. Our results showed an increased food-consumption activity in the transgenic zebrafish larva when AgRP1 neurons were photo-activated. These results indicate that the AgRP1 is an important neuron population in mediating feeding behavior in the teleost. Studying the activation and activity dynamics of these neurons in conjunction with the other hypothalamic neurons would be helpful in innovating strategies to control caloric consumption and energy homeostasis related anomalies.

Data availability

The data will be made available from the corresponding author upon request. The sequence data generated during the current study are available in the GenBank repository under the accession number PV132262. The full sequence of the AgRP1:ChR2-Kaede transgene used in this study can be accessed at https://www.ncbi.nlm.nih.gov/nuccore/PV132262.

Received: 18 December 2024; Accepted: 19 May 2025
Published online: 23 May 2025

References

1. Chen, Y., Lin, Y. C., Kuo, T. W. & Knight, Z. A. Sensory detection of food rapidly modulates arcuate feeding circuits. *Cell* **160**, 829–841 (2015).
2. Krashes, M. J. et al. Rapid, reversible activation of AgRP neurons drives feeding behavior in mice. *J. Clin. Investig.* **121**, 1424–1428 (2011).
3. Aponte, Y., Atasoy, D. & Sternson, S. M. AGRP neurons are sufficient to orchestrate feeding behavior rapidly and without training. *Nat. Neurosci.* **14**, 351–355 (2011).
4. Blanco-Centurion, C. et al. Optogenetic activation of melanin-concentrating hormone neurons increases non-rapid eye movement and rapid eye movement sleep during the night in rats. *Eur. J. Neurosci.* **44**, 2846–2857 (2016).
5. Nassi, J. J., Avery, M. C., Cetin, A. H., Roe, A. W. & Reynolds, J. H. Optogenetic activation of normalization in alert macaque visual cortex. *Neuron* **86**, 1504–1517 (2015).
6. Hagio, H. et al. Optogenetic manipulation of neuronal and cardiomyocyte functions in zebrafish using microbial rhodopsins and adenylyl cyclases. *Elife* https://doi.org/10.7554/eLife.83975 (2023).
7. Meloni, I., Sachidanandan, D., Thum, A. S., Kittel, R. J. & Murawski, C. Controlling the behaviour of Drosophila melanogaster via smartphone optogenetics. *Sci. Rep.* https://doi.org/10.1038/s41598-020-74448-4 (2020).
8. Leifer, A. M., Fang-Yen, C., Gershow, M., Alkema, M. J. & Samuel, A. D. T. Optogenetic manipulation of neural activity in freely moving Caenorhabditis elegans. *Nat. Methods* **8**, 147–152 (2011).
9. Hahn, T. M., Breininger, J. F., Baskin, D. G. & Schwartz, M. W. *Coexpression of Agrp and NPY in Fasting-Activated Hypothalamic Neurons*. http://neurosci.nature.com (1998).
10. Jeong, I. et al. mRNA expression and metabolic regulation of npy and agrp1/2 in the zebrafish brain. *Neurosci. Lett.* **668**, 73–79 (2018).
11. Shainer, I. et al. Agouti-related protein 2 Is a new player in the teleost stress response system. *Curr. Biol.* **29**, 2009-2019.e7 (2019).
12. Lin, C.-Y., Yeh, K.-Y., Lai, H.-H. & Her, G. M. AgRP neuron-specific ablation represses appetite, energy intake, and somatic growth in larval zebrafish. *Biomedicines* **11**, 499 (2023).
13. Opazo, R. et al. Fasting upregulates npy, agrp, and ghsr Without Increasing Ghrelin Levels in Zebrafish (Danio rerio) Larvae. *Front. Physiol.* https://doi.org/10.3389/fphys.2018.01901 (2019).
14. Wasserman-Bartov, T. et al. Tsh induces Agrp1 neuron proliferation in Oatp1c1-deficient zebrafish. *J. Neurosci.* **42**, 8214–8224 (2022).
15. Jeong, Y. M. et al. Optogenetic manipulation of olfactory responses in transgenic zebrafish: A neurobiological and behavioral study. *Int. J. Mol. Sci.* **22**, 7191 (2021).
16. Goodwin, N., Hernandez, R. E., Galitan, L. & Cameron, J. Until 8 days postfertilization has no impact on survival or growth through the juvenile stage. vol. 15, 515–518 (2018).
17. Thielicke, W. & Sonntag, R. Particle image velocimetry for MATLAB: Accuracy and enhanced algorithms in PIVlab. *J. Open Res. Softw.* **9**, 12 (2021).
18. Jog, C. S. *Fluid Mechanics* (Cambridge University Press, 2015).
19. Nieh, E. H., Kim, S.-Y., Namburi, P. & Tye, K. M. Optogenetic dissection of neural circuits underlying emotional valence and motivated behaviors. *Brain Res.* **1511**, 73–92 (2013).
20. Luderman, L. N., Michaels, M. T., Levic, D. S. & Knapik, E. W. Zebrafish Erc1b mediates motor innervation and organization of craniofacial muscles in control of jaw movement. *Dev. Dyn.* **252**, 104–123 (2023).
21. Paxinos, G. & Mai, J. K. Preface. In *The Human Nervous System* 2nd edn (eds Paxinos, G. & Mai, J. K.) (Academic Press, 2004). https://doi.org/10.1016/B978-012547626-3/50001-6.
22. Wang, Q. et al. Arcuate AgRP neurons mediate orexigenic and glucoregulatory actions of ghrelin. *Mol. Metab.* **3**, 64–72 (2014).
23. Denis, R. G. P. et al. Palatability can drive feeding independent of AgRP neurons. *Cell Metab.* **22**, 646–657 (2015).
24. Deem, J. D., Faber, C. L. & Morton, G. J. AgRP neurons: Regulators of feeding, energy expenditure, and behavior. *FEBS J.* **289**, 2362–2381 (2022).
25. Shainer, I. et al. Novel hypophysiotropic AgRP2 neurons and pineal cells revealed by BAC transgenesis in zebrafish. *Sci. Rep.* **7**, 44777 (2017).
26. So, W. L. et al. Ghrelin signalling in AgRP neurons links metabolic state to the sensory regulation of AgRP neural activity. *Mol. Metab.* **78**, 101826 (2023).
27. Qi, Y. et al. NPY derived from AGRP neurons controls feeding via Y1 and energy expenditure and food foraging behaviour via Y2 signalling. *Mol. Metab.* **59**, 101455 (2022).
28. Padilla, S. L. et al. Agouti-related peptide neural circuits mediate adaptive behaviors in the starved state. *Nat. Neurosci.* **19**, 734–741 (2016).
29. Engström Ruud, L., Pereira, M. M. A., de Solis, A. J., Fenselau, H. & Brüning, J. C. NPY mediates the rapid feeding and glucose metabolism regulatory functions of AgRP neurons. *Nat. Commun.* **11**, 1–12 (2020).
30. Yokobori, E. et al. Neuropeptide Y stimulates food intake in the Zebrafish, Danio rerio. *J. Neuroendocrinol.* **24**, 766–773 (2012).
31. Jeong, I. et al. Neuroscience Letters mRNA expression and metabolic regulation of npy and agrp1/2 in the zebra fish brain. *Neurosci. Lett.* **668**, 73–79 (2018).
32. Nagel, G. *et al. Channelrhodopsin-2, a Directly Light-Gated Cation-Selective Membrane Channel*. https://doi.org/10.1073/pnas.1936192100 (2003).
33. Bansal, P., Abraham, A., Garg, J. & Jung, E. E. Neuroscience research using small animals on a chip: From nematodes to zebrafish larvae. *Biochip J.* **15**, 42–51 (2021).

34. Lindken, R., Rossi, M., Große, S. & Westerweel, J. Micro-particle image velocimetry (μPIV): Recent developments, applications, and guidelines. *Lab Chip* **9**, 2551 (2009).
35. Vanwalleghem, G., Schuster, K., Taylor, M. A., Favre-Bulle, I. A. & Scott, E. K. Brain-wide mapping of water flow perception in zebrafish. *J. Neurosci.* **40**, 4130–4144 (2020).
36. Wielhouwer, E. M. et al. Zebrafish embryo development in a microfluidic flow-through system. *Lab Chip* **11**, 1815 (2011).
37. Kwon, H. J. et al. Design of a microfluidic device with a non-traditional flow profile for on-chip damage to zebrafish sensory cells. *J. Micromech. Microeng.* **24**, 017001 (2014).
38. Pekkan, K. et al. Characterization of zebrafish larvae suction feeding flow using μPIV and optical coherence tomography. *Exp. Fluids* **57**, 112 (2016).

Acknowledgements

This work was supported by the National Institute on Drug Abuse [Grant DA050962 to HM, JJ, and EEJ; Grant DA025634 to MFR], and the National Science Foundation [Grant CBET-2309589 to HM, JJ, and EEJ].

Author contributions

Conceptualization: E.E.J.; Methodology: E.E.J., H.M., and P.B.; Investigation: E.E.J., H.M., and P.B.; Formal Analysis: H.M.; Visualization: H.M., P.B., and J.J.; Imaging: Y.C., R.G., H.M., and P.B.; Microfluidic Device: H.M. and J.J.; Writing: E.E.J., H.M., and P.B.; Original Draft: H.M., and P.B.; Review and Editing: E.E.J., M.R.; Funding Acquisition: E.E.J; Resources: E.E.J.; Supervision: E.E.J.

Declarations

Competing interests

The authors declare no competing interests.

Additional information

Supplementary Information The online version contains supplementary material available at https://doi.org/10.1038/s41598-025-03040-5.

Correspondence and requests for materials should be addressed to E.E.J.